Beam characteristics measurements of neutral beam injector in Versatile Experiment Spherical Torus by using commercial smartphone camera

Yunho Jung, Soo-Ghee Oh, JongYoon Park* and Y.S. Hwang
Department of Nuclear Engineering, Seoul National University
1 Gwanak-ro, Gwanak-gu, Seoul 08826, Republic of Korea
**Corresponding author: jongblues@snu.ac.kr*

Abstract

This paper introduces a novel approach utilizing a commercial smartphone camera to measure the beam profile parameters such as size and divergence angle of the Neutral Beam Injector (NBI) in Versatile Experiment Spherical Torus (VEST). A simple and detailed image correction process is applied. The findings for the NBI operating at the beam energy of 8 keV and the beam current of 12 A include a beam height of 480 mm and a beam width of 114 mm at the beam dump, with vertical and horizontal divergence angles measured as 1.66° and 0.62°, respectively. These results agree reasonably well with the design values of the VEST-NBI system, which was designed and constructed by Korea Atomic Energy Research Institute (KAERI). This approach can be utilized as a simple beam monitoring diagnostics and extended as an advanced ion beam diagnostics for the design of new NBI systems by employing the high frame rate of smartphone cameras instead of an expensive, high-quality scientific camera.

***Keywords: Neutral Beam Injector (NBI), Beam profile, Beam divergence, Visible camera**

1. Introduction

The Neutral Beam Injector (NBI) is one of the essential parts in fusion experiments, effectively heating the plasma to achieve high performance [1]. Versatile Experiment Spherical Torus (VEST), the first and only spherical torus in Korea [2], has also operated the NBI system since 2016 [3]. Since then, to heat the VEST plasma of 170 kA, experimental studies have been actively conducted, resulting in low coupling and heating efficiency. The reason for low heating efficiency was revealed as excessive orbit losses under high beam energy conditions in the low poloidal magnetic field region of the VEST [4]. To reduce the excessive orbit losses as much as possible, the NBI system in VEST has typically operated with a low beam energy of 10 keV and ion beams current of 20 A, which is much less than its full ion beam capability of 15 keV and 40 A. Recently, VEST has successfully discharged ohmic plasma of 250 kA and 40ms, setting a new discharge record. Since the reduced first orbit loss is expected with the high plasma current of 250 kA, the operation of the new NBI(2nd) with larger beam energy is actively underway. This new beam, with its high energy (~25 keV), is expected to be utilized not only for heating, but also for beam-based diagnostics such as Charge Exchange Spectroscopy (CES), showing a high signal-to-noise ratio [5].

One important task in the development of the new NBI for VEST plasma is the design of the beamline, as recent vacuum simulation [6] results show that the inherent operational problem in the VEST NBI system might be solved with effective beamline design without significant costs. For context, here is a brief explanation. The VEST plasma has suffered from residual gas from the ion source in the NBI, impeding VEST plasma performance. One effective way to reduce residual gas flow from the NBI system is suggested as the reducing the cross-sectional area of the beamline would delay the time it takes for this residual gas to reach the main chamber. Therefore, in an experimental device where it is not possible to install numerous pumps, it is desirable to use as narrow a beamline as possible. To reduce the beamline area as much as possible, and thus reduce unwanted gas from the NBI system, it is necessary to evaluate and determine the characteristics of the ion beam such as beam size and divergence. Furthermore, this information would be useful as it directly affects the NBI operation. Obtaining this information often involves simulation work using IGUN [7] and BTR code [8] to calculate the divergence angle and beam profiles, but there have been fewer experimental measurements made so far due to limitations. For example, a calorimeter, traditionally used to measure the size of the beam, requires a relatively long extraction time due to the need to heat the target plate to a sufficiently high temperature [9]. Therefore, it is difficult to adopt for the VEST NBI, which is a pulsed system. Additionally, a typical calorimeter, which cannot adjust its position across the direction of the beam, has the disadvantage of being unable to measure the divergence angle of the beam.

In this paper, we demonstrate the measurement of the ion beam size and divergence using high-quality images captured by a smartphone camera. Moreover, since the camera image captures information from a wide range of areas, it is possible to measure not only the beam size but also the beam divergence angle by conducting proper geometric calculations. This convenient smartphone-based optical diagnosis is expected to become more widespread in field of plasma diagnostics in the future.

2. Ion beam and Measurement Setup

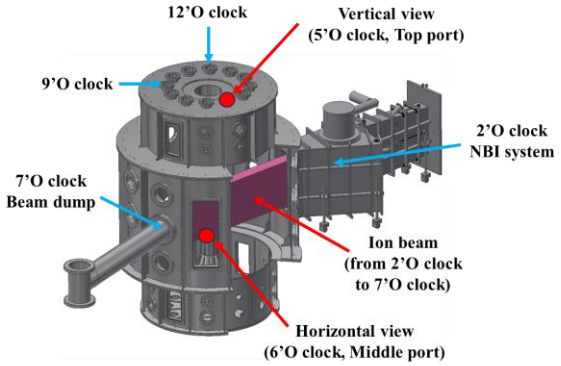

Fig. 1. Cross sectional view of VEST with NBI system. Ion beam trajectory is represented as pink block inside the chamber. Blue arrows denote direction of ports of VEST. Ports in VEST are named in clockwise order. The red dots indicate the horizontal and vertical measurement points.

Fig. 1 shows the experimental and measurement setup briefly, depicting a view of the VEST chamber, ion beam path and the position of the ports used for measurement. For the experiment in this paper, the ion beam in NBI system was operated at 8 keV, 12 A therefore total extracted power amount to 100 kW. The ion beams to be measured travel from the 2 o'clock to be dumped at 7 o'clock which is co-injected direction to ohmic plasma. Since this experiment is a beam characterization, there was no ohmic plasma in the VEST chamber during the measurement. The evolution of the simulated beam profile is shown in [3], and the beam is represented as pink in the Fig. 1. Operational conditions are the same as the typical NBI shot so far. For the measurement, the horizontal view was taken from the mid port at 6'o clock, and the vertical view was taken from the top port at 5'o clock. At these ports, the Samsung Galaxy S21+, the smartphone used in the experiments, is placed in its holder and operated with its rear wide-angle camera. The Pro video function was used to fix the shooting conditions, and the ISO was set to 100, the frame rate to 60 fps, and the shutter speed to 1/60 second. Before the operation of ion beam, the video recording function is turned on manually, then the image was selected from the recorded video. Since the light is collected for about 16.67 ms per each frame (60 fps) and the extraction time of the ion beam is 10 ms, the light generated by beam is captured in one or two frames.

3. Correction and Analysis Techniques for Images

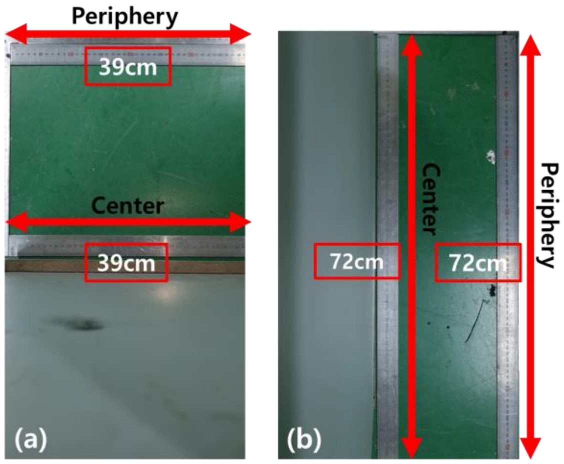

Fig. 2. Test images for checking camera distortion between center and periphery (a) Vertically (b) Horizontally.

As wide-angle camera was used, presumably, the lens distortion is expected. The images for checking the camera lens distortion were taken and shown in Fig. 2 (a) and (b). The images are taken with the same settings as the actual measurements. The smartphone was fixed parallel to the ground on a 65cm high desk, and the length of rulers in the center and periphery of the field of view was measured. As a result, almost the same values were measured in both measurements, meaning the distortion effect of the fisheye lens is very small and showing similar characteristics to a pinhole camera.

Fig. 3 shows an example case which beam is captured in two frames. Fig. 3 (a), (b), and (c) show the three frames arranged in the chronological order in a single ion beam discharge of 10ms. Fig. 3 (a) is a reference frame and serves to exclude the contribution of light emitted from the ion source other than the light generated by the beam. It is assumed that the intensity of light emitted by the ion source (mostly by hot filaments for arc discharge) is constant during these three frames. Fig. 3 (b) and (c) show a 10ms beam took over two frames. Like the case of Fig. 3 (d), Subtracted frame is generated as follows: (First frame (Fig. 3(b)) - Reference frame (Fig. 3(a))) + (Second frame (Fig. 3(c)) - Reference frame (Fig. 3(a))). If luckily have 10ms beam in one frame, the operation is simplified as follows: (First frame (Fig. 3(b) - Reference frame (Fig. 3(a)). Fig. 3 (e) is an example of subtracted frame generated from vertical view.

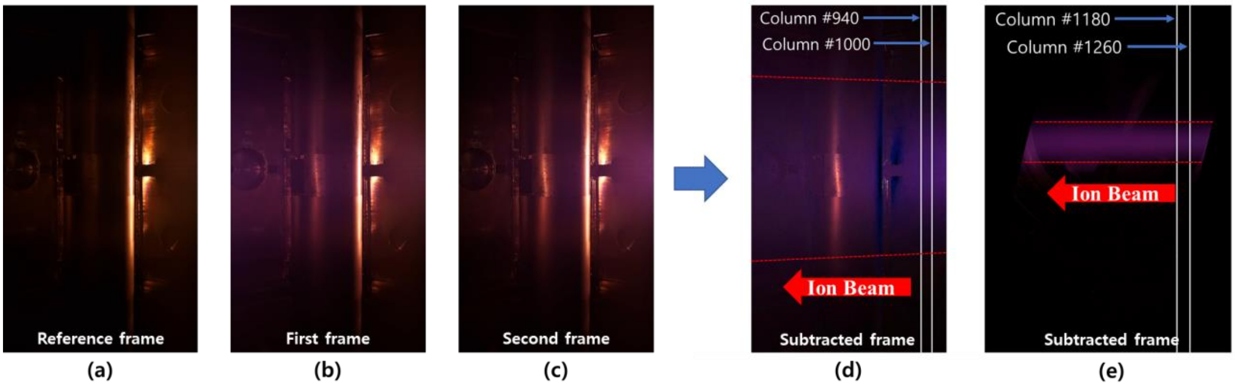

Fig. 3. Frames took from a single measurement. This case features when the 10ms beam is captured in two frames. Borderline of ion beams are denoted as red dotted lines. Intensities of white vertical lines and their gaussian fitted curves are plotted on Fig. 7. (a) Reference frame is a frame before the first emergence of the light by ion beam (b) First frame that light by beam has captured. (c) Second frame that light by beam has captured. (d) Subtracted frame (of horizontal measurement) is a frame which have get rid of effect of light from ion source. It is calculated as follows: (b)-(a) + (c)-(a). (e) Example of subtracted frame of vertical measurement.

After pre-processing with captured images, the correcting process is required to obtain ion beam size and divergence. The flow chart explaining the process of applying corrections to the initially calculated beam size from the subtracted frames is shown in Fig. 4. In step 1 and 3 of the flow charts, the beam size is calculated in raw subtracted frame based on the distance from the pixel with $1/e^2$ the intensity to the pixel with the maximum intensity.

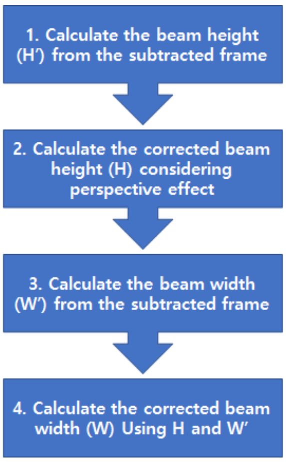

Fig. 4. Flow chart for correcting beam height and width obtained from each subtracted frame.

In the step 2 of the flow chart, perspective effect should be considered to correct the beam height calculated in the step 1. Fig. 5 shows how much this effect occurs. The cyan lines show the angle of view of the horizontal view as seen from the top view. In addition, the distance between the camera located in the horizontal view and the center of the beam is constantly changing, so a correction must be made to account this. For example, there are three intersections of the cyan lines with the middle red line that represents the center of the beam. The perpendicular distances to those three points from the camera are 388 mm, 507 mm, and 733 mm from the left, respectively.

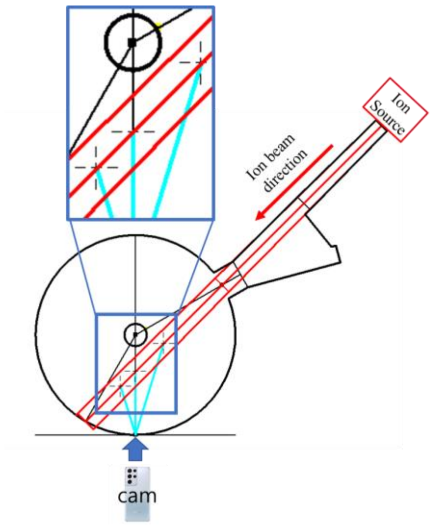

Fig. 5. Schematic top view of VEST chamber. The red lines denote ion beam. The cyan lines indicate the horizontal view itself and distance from the center of the beam to camera, which should be considered when calculating the beam height.

Similarly, we calculate the beam width from the subtracted frame obtained by shooting in the vertical direction (step 3 of the flow chart in Fig. 4). Since this calculated width from vertical view is a result of accumulated light in height, the width contribution should be calculated with known values. Through simple geometry and equating, corrected width can be calculated as follows:

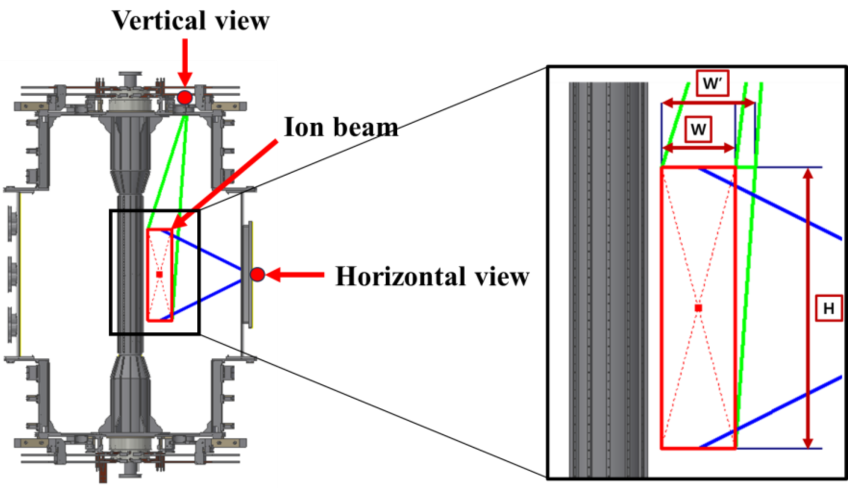

Fig. 6. Vertical cross-sectional view of VEST and magnified view to denote parameters to calculate corrected beam width. (W is corrected beam width, W' is beam width calculated from raw subtracted frame, H is corrected beam height and H' is beam height calculated from raw subtracted frame)

$$(1)\ \ W = \frac{1230W' + \frac{HW'}{2} - 193H}{1230} \text{ (in millimeters)}$$

where W is corrected beam width, W' is beam width calculated from raw subtracted frame, H is corrected beam height and H' is beam height calculated from raw subtracted frame. Rational numbers in Eq. (1) have come from values in the VEST chamber geometry which is distance from the center of the beam to Vertical view (vertically 1230 mm and horizontally 193 mm). The difference between W and W' is shown in Fig. 6.

4. Results and Discussion

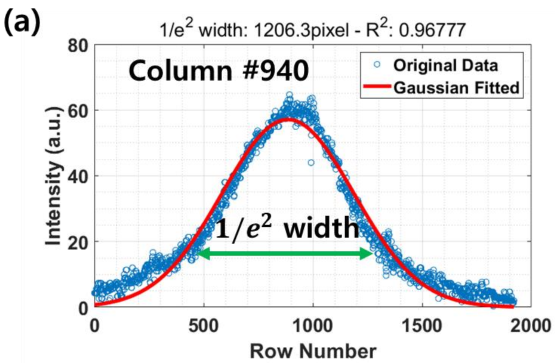

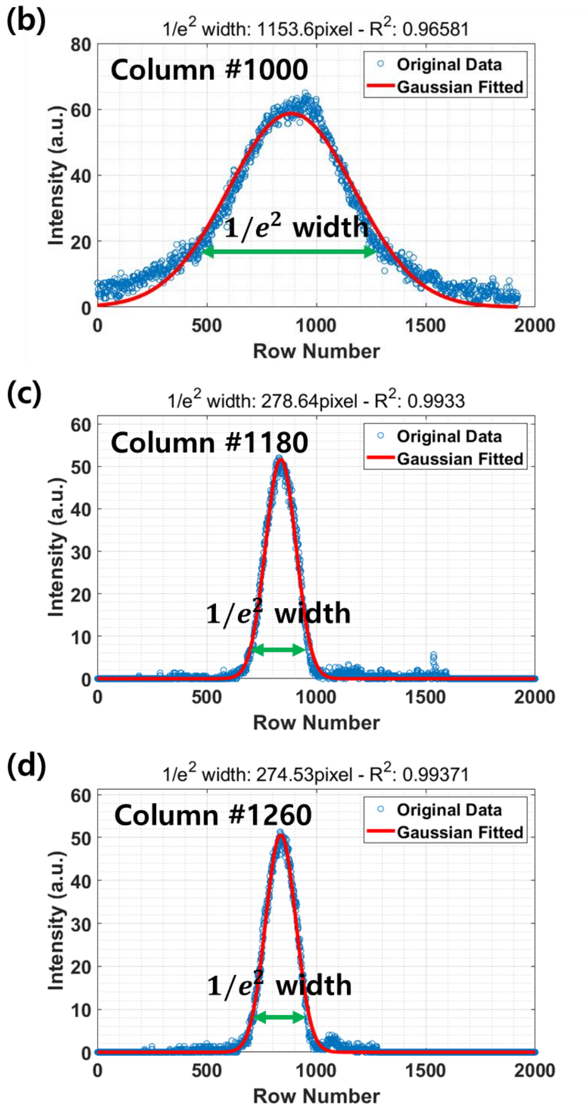

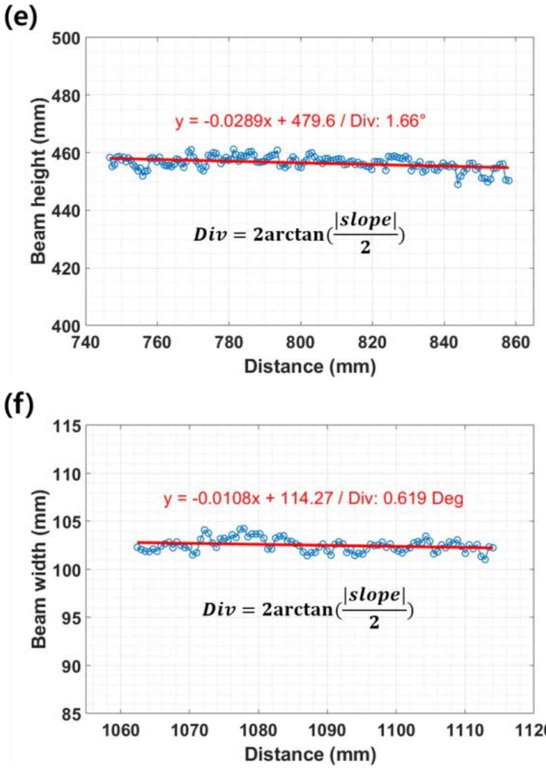

Fig. 7. Results of gaussian fitting and their original data in each subtracted frame. (a) Column number 940 in horizontal subtracted frame. (b) Column number 1000 in horizontal subtracted frame. (c) Column number 1180 in vertical subtracted frame. (d) Column number 1260 in vertical subtracted frame. (e) Corrected beam height with distance from beam dump. Vertical divergence is calculated from the trend of beam height. (f) Corrected beam width with distance from beam dump. Horizontal divergence is calculated from the trend of beam width.

Fig. 7 (a)-(d) show the original data and the gaussian fitted results on example columns of the subtracted frame obtained from the horizontal and vertical view, respectively. It can be seen that the smaller the column number, the larger the calculated beam size because it is close to the beam dump at 7 o'clock. Fig. 7 (e) and (f) are the results of the calculated beam size after correcting the errors corresponding to the step 2 and 4 of the flow charts in Fig. 4, respectively. As expected, both beam height and width show a gradual increase as the distance decreases. Distance is calculated with the beam dump at 7 o'clock as the origin, resulting in a linear fitted equation with a negative slope. This seems reasonable given the spreading nature of the ion beam. Divergence angle of each case is calculated using the simple equation in Fig. 7 (e) and (f). Finally, the measured $1/e^2$ sized beam parameters of VEST NBI on 8 keV, 12 A are summarized in Table. 1. These results are in good agreement with the results of the simulation conducted at KAERI.

Table I: $1/e^2$ sized ion beam parameter of VEST NBI on 8 keV, 12 A output

$1/e^2$ sized beam parameter	Measurement by Smartphone Camera	Simulation By KAERI [3]
Height at beam dump	480mm	570mm
Width at beam dump	114mm	179mm
Vertical divergence	1.66°	2.0°
Horizontal divergence	0.62°	1.0°

5. Conclusion

Beam size and divergence angles of an 8 keV, 12 A ion beam from the VEST NBI was successfully measured using camera in smartphone. It is noteworthy that even though there are cases of measuring beam size and divergence angles using optical cameras before [10], there is no precedent for using a commercial smartphone for the measurements. Since diagnostics using commercial smartphones requires less cost and effort than using another traditional optical diagnostics, future advances in visible plasma diagnostics in accordance with the improvement of smartphone camera are expected.

The successful measurements provided a basis for the design of the new NBI beamline. NBI parameters that have been difficult to measure in the past were measured in a relatively convenient way, and an attractive measurement method is proposed that is somewhat consistent with simulation results from KAERI in the past. This work was necessary for the beamline design, which is now underway with the results above. It is expected to result in a beamline with an optimized cross-sectional area.

In the measurement, all of the optical information by ion beam was captured in a single frame to estimate the average parameters over the entire 10 ms extraction time. However, given that commercial smartphone cameras support high frame rate shooting modes (up to 960 fps), there are future plans to utilize this capability to determine trends over time. As mentioned above, it is expected that this measurement method can be actively used not only in the development of the new NBI but also in the other fusion relevant system.

Acknowledgment

This work was supported by the National Research Foundation of Korea (NRF) grant funded by the Korean government (MSIT) (No. 2021M3F7A1084418).

REFERENCES

[1] Speth, E. "Neutral beam heating of fusion plasmas." Reports on Progress in Physics 52.1 (1989): 57.

[2] Chung, K. J., *et al.* "Design features and commissioning of the versatile experiment spherical torus (VEST) at Seoul National University." *Plasma Science and Technology* 15.3 (2013): 244.

[3] Kim, T. S., et al. "Conceptual design of NBI beamline for VEST plasma heating." *Fusion Engineering and Design* 109 (2016): 411-415.

[4] Lee, Kihyun, et al. "IMPROVEMENT OF NEUTRAL BEAM INJECTION HEATING EFFICIENCY BY REDUCING THE FIRST ORBIT LOSS IN VERSATILE EXPERIMENT SPHERICAL TORUS."

[5] Kim, YooSung, et al. "Design of combined system of helium charge exchange spectroscopy and hydrogen beam emission spectroscopy in VEST." Fusion Engineering and Design 123 (2017): 975-978.

[6] Jung, Yunho. "Study of Neutral Pressure Evolution during Gas Puffing in VEST using Molflow+" KAPRA & KPS/DPP Conference, 29-30 June 2023, Seoul, Poster Presentation.

[7] Becker, Reinard, and W. B. Herrmannsfeldt. "i g u n− A program for the simulation of positive ion extraction including magnetic fields." Review of scientific instruments 63.4 (1992): 2756-2758.

[8] Oh, B. H., and E. D. Dlougach. "Beam transport code for the KSTAR NB heating system." 20th IEEE/NPSS Symposium onFusion Engineering, 2003.. IEEE, 2003.

[9] Chiu, Henry. "Measurement of neutral beam profiles at DIII-D." *Fusion technology* 34.3P2 (1998): 564-567.

[10] Ugoletti, M., et al. "Visible cameras as a non-invasive diagnostic to study negative ion beam properties." Review of Scientific Instruments 92.4 (2021).